PROCEEDINGS OF SCIENCE

# Characteristic emission of star-forming high redshift galaxies: testing the IR template

**J. Bogdanoska**[a,*] **and D. Burgarella**[b]

[a] *Ss. Cyril and Methodius University in Skopje*

[b] *Aix Marseille Univ, CNRS, CNES, LAM, Marseille*

*E-mail:* janabogdanoska@pmf.ukim.mk, denis.burgarella@lam.fr

In anticipation of JWST data, today's study of early Universe galaxies focuses on preparations for efficient data handling. For that reason, in our previous work (Burgarella et al. 2022), we constructed an IR template which is based mainly on the ALPINE data sample with an addition of a few other well-studied galaxies, which includes galaxies in the redshift range $4.5 < z < 6.2$. To build the IR template, a sample of galaxies with a well-sampled SED was chosen and SED fitting was performed on the entire sample using the flux data of all available filters. This mainly served to constrain the UV part of the SED, give an idea about the type of IR SED that we might expect, and have a best-fit model of the entire SED. Then, by normalising the SEDs of each individual galaxy at the rest-frame 200 $\mu$m flux, a composite IR SED was constructed from the normalised ALMA Band 6 or 7 fluxes of all galaxies, this time in the observer frame. When shifted to the observer frame, the flux of the ALMA Bands is at a different wavelength for each galaxy, due to the difference in redshift. We call this technique "using the Universe as a spectrograph". Finally, these data points were fitted to create a SED template representative of the entire studied sample. The IR template is expressed through the parameters of three different dust emission models that are required as input in the SED fitting code CIGALE which we consistently use in our work. By using these values of the parameters, the number of models needed to fit the SED is greatly reduced. In this work, we use older data from Bouwens et al. (2016) to test the IR template. Three of the objects from this dataset were already used in building the IR template, however, the majority of them did not meet the required minimum of 5 data points in the UV-optical and the S/N > 1.5 criteria. The SED fitting with CIGALE is first carried out by using a grid of models for dust emission. In a second fitting run, the parameters of the IR template are used. We compare the main output parameters of the models, i.e. the characteristics of the galaxies, as well as the typical diagnostic diagrams for this kind of sample, such as the SFR-$M_{star}$, IRX-$M_{star}$ and IRX-$\beta_{UV}$ diagrams.

*11th International Conference of the Balkan Physical Union (BPU11),*
*28 August - 1 September 2022*
*Belgrade, Serbia*

*Speaker





PoS(BPU11)042

## 1. Introduction

Answering the questions pertaining to the evolution of galaxies requires understanding the dust within them and the cycles it undergoes. As the observing capabilities grow, so does science dive deeper into the history of the Universe, probing the earliest type galaxies at the epoch of reionization (EoR) at redshifts $z > 5$. Even though this journey of discovery has begun decades ago [1] with the study of high-redshift Lyman Break Galaxies (LBGs), the question of the far-infrared (far-IR) emission of galaxies is still open. Many advancements have been made due to the powerful observatories, such as the Herschel space observatory (Herschel), the Atacama Large Millimeter/Submillimeter Array (ALMA), and the Northern Extended Millimeter Array (NOEMA), as well as the hard work of many scientific groups [2–11, and many others].

One of the main tools used to study the galaxy parameters is Spectral Energy Distribution (SED) fitting, a method that uses observations in a wide range of bands and compares the measured fluxes to ones estimated by models. The SED fitting models include information about the synthetic stellar population, as well as prescriptions for dust absorption and emission where infrared (IR) data is available. Information about the properties and history of the stellar population is contained within the ultraviolet (UV) part of the SED, while the IR emission is generally associated with the dust emission, primarily the thermal continuum radiation of the dust grains [12]. For more details on SED fitting, we refer to the review by Conroy [13]. In this work, the SED fitting is consistently performed by the code CIGALE[1] [14–16]. Below we mention some of the main parameters used in this work that can be extracted with SED fitting, with their definitions and common ways of estimating.

The galaxy's stellar mass, which represents the total mass of stars contained in the galaxy is estimated using the mass-to-light ratio, multiplied by a measured near-IR (NIR) luminosity:

$$\frac{M_*}{L_{\rm NIR}} = 0.6\frac{M_\odot}{L_\odot}, \tag{1}$$

where the $L_{\rm NIR}$ is commonly at 1.65$\mu$m [17, H band], 2.15$\mu$m [18, K band], or 3.6$\mu$m [19].

The stellar mass and SFR are output parameters in the SED fitting codes, and they are estimated through the SSP templates and Initial Mass Function (IMF) assumed during the fitting.

The SFR is usually determined with the use of a classical calibration [20]. In the UV continuum (between 1250 and 2500 Å) young stars dominate, and this luminosity can be converted to SFR with the following calibration relation, derived from stellar population synthesis:

$$\mathrm{SFR}(M_\odot \mathrm{yr}^{-1}) = 1.4 \times 10^{-28} L_\nu (\mathrm{ergs}^{-2}\mathrm{Hz}^{-1}) \tag{2}$$

Finally, a quantity called Infrared Excess (IRX) is used in this work, and its purpose is to serve as a proxy for estimating the dust attenuation in a galaxy. It is defined as [21]:

$$\mathrm{IRX} = \log \frac{L(\mathrm{TIR})}{L(\mathrm{FUV})} \tag{3}$$

[1] https://cigale.lam.fr/

Here, $L(\mathrm{TIR})$ represents the total infrared luminosity, and $L(\mathrm{FUV})$ is the FUV luminosity at 1600 Å.

In practice, accurately modelling the dust emission of high redshift galaxies is not a simple matter, especially if we are interested in the particulars of individual objects. Combining several objects to account for the less-than-ideal accuracy and narrow wavelength coverage currently available for such faint objects is one approach that has been used in the literature [22–24]. Starting from the assumption that the sample of galaxies chosen has a common characteristic dust emission, it is possible to build a template that will be representative of the sample and which will improve the assumptions we make when faced with a lack of data.

As new facilities become available to observe distant galaxies, the number of objects for which we have data increases. Fitting the SEDs of a large number of sources requires significant computational time, and this can become quite expensive when we are trying to achieve better accuracy of our results. This is another aspect of why building IR templates is important; they are a technique that could possibly reduce the computational time necessary to extract quality information from our observations. This work is the continuation of the Burgarella et al. (2022, [25], B22 henceforth) paper, where one such IR template was proposed. Our aim is to test the template on a completely different data set and determine how efficient it would be in larger, more model-heavy SED fitting runs. In this paper, we assume a Chabrier initial mass function [IMF, 26]. We use WMAP7 cosmology [27].

## 2. The sample of studied galaxies

Two different galaxy samples are relevant to this work. The first sample of galaxies is the basis of the IR template and it is described in B22. The data used to construct the template mainly consists of ALPINE data [8, 28, 29], combined with a few other sources collected from various works and presented in [9]. The ALPINE sample was chosen because it falls in the redshift range $4.5 < z < 5.5$, and is representative of high redshift Star-Forming Galaxies (SFGs). They have been determined to be located on or near the main sequence of the SFR-$M_{star}$ diagram for their appropriate redshifts [30, 31], and the sample is dominated by UV-selected galaxies.

The ALPINE sample of 118 objects was not used in its entirety, but only as a sub-sample with the best-quality data. The final sample consists of 27 objects with ALMA detections, while the 78 ALMA upper limits were used in later stages after the first version of the template was created and tested for homogeneity. The rest were not used due to a lack of UV-optical-near-IR range data. Generally, the objects that were included in the final sample were the ones that fulfilled the following selection conditions:

- ALMA band 7 or band 6 detection with S/N > 3
- ALMA band 7 upper limits (for the second version of the template)
- SFGs with more than 5 bands in the UV and optical
- UV-optical-IR detections with S/N > 2.5
- [CII]158$\mu$m measurement

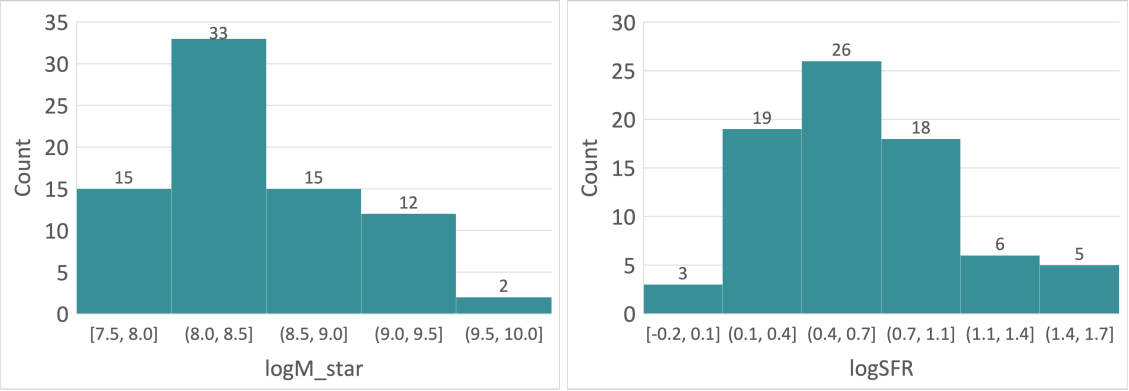


**Figure 1:** A histogram of the B16 data, binned by stellar masses (left panel) and SFR (right panel), used to verify the homogeneity of the sample.

The second sample used in this work is the data on which we test the IR template. It is the dataset presented in Bouwens et al. (2016, [2], B16 henceforth). We have taken the flux data directly so that we are better able to compare the results from the SED fitting, as opposed to taking the parameter values estimated in [2] using a different SED fitting software. It should be noted that the B16 data was considered in the work of B22, however, none of the objects satisfied the selection criteria described above. The B16 data comprises of HST and ALMA band 6 observations of high-redshift SFGs within the Hubble Ultra Deep Field (HUDF) and it is composed of 78 galaxies from within the redshift range of $z \approx 4 - 10$. Histograms of the sample per stellar mass and SFR are shown in Fig. 1.

## 3. Method

As this paper is based on the B22 work, a simplified summary follows. The relevant goal of the B22 paper was to find an IR template that is representative of star-forming galaxies in the early Universe. Once the sample was selected, SED fitting was performed in a few phases in the following order:

1. Fit the SEDs of the entire sample using all of the available data
2. Normalise the flux observations of each object with the rest-frame 200 $\mu$m flux obtained from the best-fit SED of step 1
3. Construct a composite IR SED from the normalised ALMA Band 6 or 7 fluxes of all galaxies, each shifted to the observer frame. This way, the ALMA flux of each object is at a slightly different wavelength, due to the differences in redshift. This method is referred to as "Using the Universe as a spectrograph"
4. Fit the composite IR SED as if it were the SED of a single object
5. The best-fit model of the composite IR SED becomes the template which is representative of the entire studied sample.

The template is given both as flux values for rest-frame wavelengths, and as a set of input parameters that were used in CIGALE to give the best-fitting SED. We use the latter in the work presented below, specifically the values for the DL2014 dust emission model, their values being:

$$q_{PAH} = 0.47 \tag{4}$$
$$\alpha = 2.39 \pm 0.44 \tag{5}$$
$$u_{min} = 18.1 \pm 12.7 \tag{6}$$
$$\gamma = 0.54 \pm 0.35 \tag{7}$$

We use these values to test the IR template of B22. We fit our SEDs with both the average values given here, as well as with 2 or 3 values within the error bars, with no significant difference. In fact, in this work we only perform the first part of Step 1 above on our sample of galaxies, we fitted the SED with CIGALE without concerning ourselves with the IR dust emission. All CIGALE models and input parameters are the same as the ones used in B22, except the dust emission model.

Testing the template requires determining the galaxy parameters in a trustworthy way for comparison. For this purpose, we perform a second SED fitting in our usual manner, meaning we test the full range of dust emission model parameters. The galaxy parameters obtained this way are denoted as "all models" on the plots in Fig. 2. The only difference between the input parameters of both the "all models" and the "IR template" SED fitting runs is in the dust emission models, so any differences we find in the results should be due to the assumptions we make on the dust emission.

## 4. Analysis of the results

To estimate the method, we start by making assumptions on what type of objects is expected from the selection criteria. Then, an analogy with what we know about this galaxy type allows us to check that we are in agreement, with the expected results. Firstly, we directly compare the results of the SED fitting with the IR template to our "usual" SED fitting scheme. Secondly, we examine the main diagnostic tools, which would enable us to compare our results to standards that have been studied widely in the literature.

The first comparison is presented in Fig. 2. The three main parameters are shown, the stellar mass of the galaxies, the SFR and the IRX. We can see that the stellar mass is significantly closer to the 1:1 line compared to the other two parameters. What is noticeable about all three plots is that even though some correlation can be noticed, the scatter is quite significant.

To quantify the scatter we examine the difference between the parameter values, defined as $\Delta P = P_{all} - P_{template}$, where $P$ stands for each of the parameters ($\log M$, SFR or IRX), and the subscripts $all$ and $template$ refer to the parameter obtained when the fitting was performed with the full range of models and the IR template, respectively. For the stellar masses, 56 objects (72%) have a difference $\Delta P_{\log M_{star}} < 0.3$dex and 32 objects (41%) have a difference $\Delta P_{\log M_{star}} < 0.1$dex. Conversely, for the SFR only 12 objects (15%) have a difference $\Delta P_{\log SFR} < 0.3$dex and this value goes as low as 4 objects (5%) for a difference of $\Delta P_{\log SFR} < 0.1$dex. The situation is similar, though slightly better for the IRX, with the counts being 41 objects (52%) for a difference

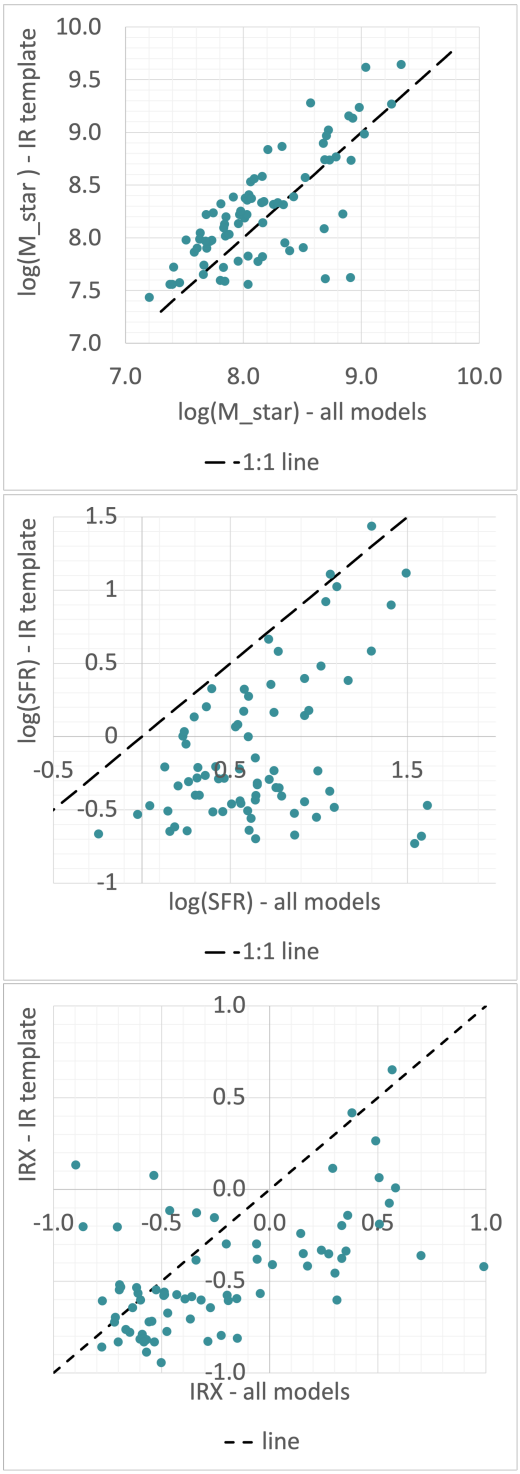


**Figure 2:** Comparison plots between the SED fitting results obtained by running a full range of models (all models) and by running a reduced number of models, where the dust emission parameters are taken from the template by B22 (IR template). The top panel represents the stellar masses, the middle is the star formation rate and the bottom is the infrared excess. On each, a $x = y$ line is shown to mark the deviation of the values for each parameter.

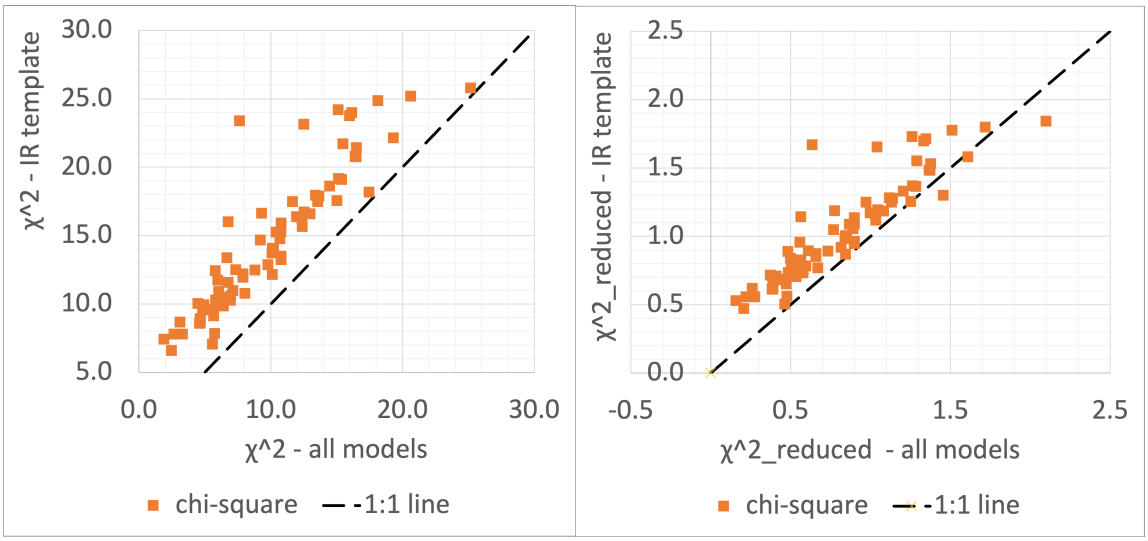


**Figure 3:** Comparison of the best-fit $\chi^2$ of the SED fitting results obtained by running a full range of models (all models) and by using the template by B22 (IR template). The left panel represents the $\chi^2$ and the right is the reduced $\chi^2$.

$\Delta P_{IRX} < 0.3$dex and 16 objects (21%) for $\Delta P_{IRX} < 0.1$dex. This confirms what was expected from a visual inspection of the plots, the discrepancy between the results is quite significant.

For a final direct comparison between these two differently obtained results of the same objects, we compare the $\chi^2$ and the reduced $\chi^2$ of both, as shown in Fig. 3. The difference is quite dramatic between the two $\chi^2$ estimates, with an average difference $\chi^2_{all} - \chi^2_{template} = 4.6$ (Fig. 3, left). The reduced $\chi^2$ seems a lot better, $\chi^2_{all,reduced} - \chi^2_{template,reduced} = 0.23$ on average (Fig. 3, right). This apparent improvement is expected because the reduced $\chi^2$ takes into account the difference in free parameters in the models. However, even the difference in absolute $\chi^2$ seems less substantial if we consider that the objects have a high $\chi^2$ to start, which is of little wonder considering the data we used was below the quality standards of B22.

Except for testing our method internally with two similar SED fitting methods, we check whether the results we get are in accordance with what is found in the literature. Using the galaxy parameters from the SED fitting with the IR template, we build some of the classical diagnostic plots for our sample. We show the location of our data on a SFR-$M_{star}$ diagram, an IRX-$M_{star}$ diagram and a IRX-$\beta_{UV}$ (defined in e.g. [32]).

The top panel of Fig. 4 represents the SFR-$M_{star}$ diagram, and as expected since our sample is built from SFGs, our objects lie near the main sequence. The comparison is made to the following equation by Pearson et al. (2018) [31]:

$$\log(SFR) = (1.00 \pm 0.22)(\log(M_{star}) - 10.6) + (1.92 \pm 0.21) \tag{8}$$

The IRX-$M_{star}$ relation is presented on the middle panel of Fig. 4. This one is very relevant to our investigation, as the IRX serves as a proxy for dust attenuation. We use the "consensus" relation of [2], even though more recent updates on this relation exist. The main reasoning is that many

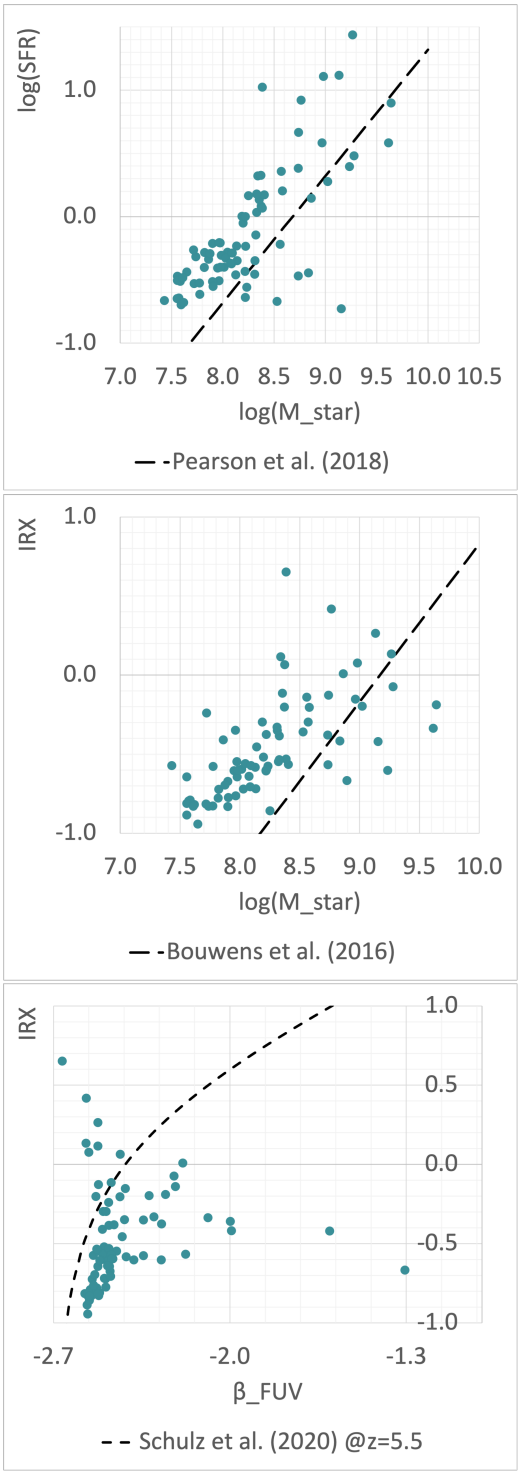


**Figure 4:** Diagnostic plots representing some of the main relations the objects of our sample are expected to follow. The top panel represents the relation between the stellar mass and star formation rate, the middle panel shows the dependence of the IRX on the stellar mass, and the bottom is the relationship between the IRX and the UV slope $\beta$. The dashed lines represent literature relations for comparison, the equations are given in the text.

of these works find a redshift dependence of this relation [33, 34], while our sample has not been divided by redshift and spans a significant redshift range. The consensus relation is the following:

$$\log_{10}(IRX) = \log_{10}(M_{star}/M_{\odot}) - 9.17 \tag{9}$$

Finally, the bottom panel shows the relationship between the IRX and the UV slope $\beta_{UV}$. Here we also encounter the issue of the redshift dependence of this relation, nevertheless, we use a relation estimated for a given redshift of $z = 5.5$. The relation is that of Schulz et al. (2020) [35]. We can see that most of our data is within the expected range, with some outliers which are to be expected. The relation is the following:

$$IRX = \log_{10}(1.68) + \log_{10}(10^{(0.4)(3.85+1.95(\beta+\beta_z))} - 1) \tag{10}$$

$$\beta_z = 0.142z - 0.081 \tag{11}$$

## 5. Conclusions

Modelling the IR dust emission of distant galaxies is quite difficult, even with the aid of state-of-the-art facilities. To achieve better results, we can combine as much available data as possible to better understand the properties and processes ongoing in these early Universe galaxies. For that purpose, B22 propose an IR template that can be used to model the dust emission, especially when little to no data is available. The mission of this work was to test the proposed template and to estimate whether or not it is a reasonable assumption to be made in future work. From our investigations we can point out the following:

- Fitting the SED with and without a template gives relatively different results, however, the diagnostic plots obtained are still within the expected range
- The $\chi^2$ of the fit is worse when using the template, but the difference in the reduced $\chi^2$ is not so significant. The loss in the goodness of fit seems less significant if we also look at the absolute values of the $\chi^2$, which are very high for both fits
- The computational time was reduced significantly, as the SED fitting runs with the template took around 1-2 hours on a personal laptop, while the full models fitting would be completely impossible on such a modest machine

The current reality is that it is not uncommon when fitting the IR SED, to only have a single data point in this range. Given the lack of options, having a template as a "prior" to input in the SED fitting models is as good of a starting point as any. As the results shown previously suggest, the IR template presented by B22 may not be an ideal solution, but it does provide useful results, especially when faced with the usual lack of more detailed data. This means that the proposed template can serve as a foundation stone which can and will be further improved as similar galaxies are studied in more detail, and our knowledge of the overall processes ongoing in galaxies becomes better understood.

## References


[1] P. Madau, *Radiative Transfer in a Clumpy Universe: The Colors of High-Redshift Galaxies*, *The Astrophysical Journal* **441** (1995) 18.

[2] R.J. Bouwens, M. Aravena, R. Decarli, F. Walter, E. da Cunha, I. Labbé et al., *ALMA Spectroscopic Survey in the Hubble Ultra Deep Field: The Infrared Excess of UV-Selected z = 2-10 Galaxies as a Function of UV-Continuum Slope and Stellar Mass*, *The Astrophysical Journal* **833** (2016) 72.

[3] A. Ferrara, H. Hirashita, M. Ouchi and S. Fujimoto, *The infrared-dark dust content of high redshift galaxies*, *Monthly Notices of the Royal Astronomical Society* **471** (2017) 5018.

[4] T. Hashimoto, A.K. Inoue, K. Mawatari, Y. Tamura, H. Matsuo, H. Furusawa et al., *Big Three Dragons: A z = 7.15 Lyman-break galaxy detected in [O III] 88 mum, [C II] 158 mum, and dust continuum with ALMA*, *Publications of the Astronomical Society of Japan* **71** (2019) 71.

[5] C. Behrens, A. Pallottini, A. Ferrara, S. Gallerani and L. Vallini, *Ly alpha emission from galaxies in the Epoch of Reionization*, *Monthly Notices of the Royal Astronomical Society* **486** (2019) 2197.

[6] M.P. Koprowski, K.E.K. Coppin, J.E. Geach, U. Dudzevičiūtė, I. Smail, O. Almaini et al., *An ALMA survey of the SCUBA-2 cosmology legacy survey UKIDSS/UDS field: Dust attenuation in high-redshift Lyman-break galaxies*, *Monthly Notices of the Royal Astronomical Society* **492** (2020) 4927.

[7] A.L. Faisst, Y. Fudamoto, P.A. Oesch, N. Scoville, D.A. Riechers, R. Pavesi et al., *ALMA characterizes the dust temperature of z = 5.5 star-forming galaxies*, *Monthly Notices of the Royal Astronomical Society* **498** (2020) 4192.

[8] A.L. Faisst, D. Schaerer, B.C. Lemaux, P.A. Oesch, Y. Fudamoto, P. Cassata et al., *The ALPINE-ALMA [C II] Survey: Multiwavelength Ancillary Data and Basic Physical Measurements*, *The Astrophysical Journal Supplement Series* **247** (2020) 61.

[9] D. Burgarella, A. Nanni, H. Hirashita, P. Theulé, A.K. Inoue and T.T. Takeuchi, *Observational and theoretical constraints on the formation and early evolution of the first dust grains in galaxies at 5 < z < 10*, *Astronomy and Astrophysics, Volume 637, id.A32, 16 pp.* **637** (2020) A32.

[10] Y. Sugahara, A.K. Inoue, T. Hashimoto, S. Yamanaka, S. Fujimoto, Y. Tamura et al., *Big Three Dragons: A [N II] 122 mum Constraint and New Dust-continuum Detection of a z = 7.15 Bright Lyman-break Galaxy with ALMA*, *The Astrophysical Journal* **923** (2021) 5.

[11] S. Schouws, M. Stefanon, R. Bouwens, R. Smit, J. Hodge, I. Labbé et al., *Significant Dust-obscured Star Formation in Luminous Lyman-break Galaxies at z 7-8*, *The Astrophysical Journal* **928** (2022) 31.

[12] B.T. Draine, *Interstellar Dust Grains*, *Annual Review of Astronomy andAstrophysics, vol. 41, pp.241-289* **41** (2003) 241.

[13] C. Conroy, *Modeling the Panchromatic Spectral Energy Distributions of Galaxies*, *Annual Review of Astronomy and Astrophysics, vol. 51, issue 1, pp. 393-455* **51** (2013) 393.

[14] M. Boquien, D. Burgarella, Y. Roehlly, V. Buat, L. Ciesla, D. Corre et al., *CIGALE: a python Code Investigating GALaxy Emission*, *Astronomy and Astrophysics, Volume 622, id.A103, 33 pp.* **622** (2019) A103.

[15] S. Noll, D. Burgarella, E. Giovannoli, V. Buat, D. Marcillac and J.C. Muñoz-Mateos, *Analysis of galaxy spectral energy distributions from far-UV to far-IR with CIGALE: studying a SINGS test sample*, *Astronomy and Astrophysics, Volume 507, Issue 3, 2009, pp.1793-1813* **507** (2009) 1793.

[16] D. Burgarella, V. Buat and J. Iglesias-Páramo, *Star formation and dust attenuation properties in galaxies from a statistical ultraviolet-to-far-infrared analysis*, *Monthly Notices of the Royal Astronomical Society* **360** (2005) 1413.

[17] L. Ciesla, M. Boquien, A. Boselli, V. Buat, L. Cortese, G.J. Bendo et al., *Dust spectral energy distributions of nearby galaxies: an insight from the Herschel Reference Survey*, *Astronomy and Astrophysics, Volume 565, id.A128, 33 pp.* **565** (2014) A128.

[18] E.F. Bell, D.H. McIntosh, N. Katz and M.D. Weinberg, *The Optical and Near-Infrared Properties of Galaxies. I. Luminosity and Stellar Mass Functions*, *The Astrophysical Journal Supplement Series* **149** (2003) 289.

[19] D.O. Cook, D.A. Dale, B.D. Johnson, L. Van Zee, J.C. Lee, R.C. Kennicutt et al., *Spitzer Local Volume Legacy (LVL) SEDs and physical properties*, *Monthly Notices of the Royal Astronomical Society* **445** (2014) 899.

[20] R.C. Kennicutt, *Star Formation in Galaxies Along the Hubble Sequence*, *Annual Review of Astronomy and Astrophysics, Volume 36, 1998, pp. 189-232.* **36** (1998) 189.

[21] C.-N. Hao, R.C. Kennicutt, B.D. Johnson, D. Calzetti, D.A. Dale and J. Moustakas, *Dust-corrected Star Formation Rates of Galaxies. II. Combinations of Ultraviolet and Infrared Tracers*, *The Astrophysical Journal* **741** (2011) 124.

[22] M. Ouchi, T. Yamada, H. Kawai and K. Ohta, *Expected Submillimeter Emission and Dust Properties of Lyman Break Galaxies at High Redshift*, *The Astrophysical Journal* **517** (1999) L19.

[23] A.E. Shapley, C.C. Steidel, M. Pettini and K.L. Adelberger, *Rest-Frame Ultraviolet Spectra of z~3 Lyman Break Galaxies*, *The Astrophysical Journal* **588** (2003) 65 [astro-ph/0301230].

[24] E.A. Pearson, S. Eales, L. Dunne, J. Gonzalez-Nuevo, S. Maddox, J.E. Aguirre et al., *H-ATLAS: estimating redshifts of Herschel sources from sub-mm fluxes*, *Monthly Notices of the Royal Astronomical Society* **435** (2013) 2753 [1308.5681].

[25] D. Burgarella, J. Bogdanoska, A. Nanni, S. Bardelli, M. Béthermin, M. Boquien et al., *The ALMA-ALPINE [CII] survey. The star formation history and the dust emission of star-forming galaxies at 4.5 < z < 6.2*, *Astronomy and Astrophysics, Volume 664, id.A73, 39 pp.* **664** (2022) A73.

[26] G. Chabrier, *Galactic Stellar and Substellar Initial Mass Function*, *Publications of the Astronomical Society of the Pacific* **115** (2003) 763 [astro-ph/0304382].

[27] E. Komatsu, K.M. Smith, J. Dunkley, C.L. Bennett, B. Gold, G. Hinshaw et al., *Seven-year Wilkinson Microwave Anisotropy Probe (WMAP) Observations: Cosmological Interpretation*, *The Astrophysical Journal Supplement* **192** (2011) 18 [1001.4538].

[28] O. Le Fèvre, M. Béthermin, A. Faisst, G.C. Jones, P. Capak, P. Cassata et al., *The alpine-alma [cii] survey. survey strategy, observations, and sample properties of 118 star-forming galaxies at 4 < z < 6*, *Astronomy and Astrophysics* **643** (2020) A1 [1910.09517].

[29] M. Béthermin, Y. Fudamoto, M. Ginolfi, F. Loiacono, Y. Khusanova, P.L. Capak et al., *The ALPINE-ALMA [CII] survey: Data processing, catalogs, and statistical source properties*, *Astronomy and Astrophysics* **643** (2020) A2 [2002.00962].

[30] J.S. Speagle, C.L. Steinhardt, P.L. Capak and J.D. Silverman, *A Highly Consistent Framework for the Evolution of the Star-Forming "Main Sequence" from z ~0-6*, *The Astrophysical Journal Supplement* **214** (2014) 15 [1405.2041].

[31] W.J. Pearson, L. Wang, P.D. Hurley, K. Małek, V. Buat, D. Burgarella et al., *Main sequence of star forming galaxies beyond the Herschel confusion limit*, *Astronomy and Astrophysics* **615** (2018) A146.

[32] D. Calzetti, A.L. Kinney and T. Storchi-Bergmann, *Dust Extinction of the Stellar Continua in Starburst Galaxies: The Ultraviolet and Optical Extinction Law*, *The Astrophysical Journal* **429** (1994) 582.

[33] Y. Fudamoto, P.A. Oesch, A. Faisst, M. Béthermin, M. Ginolfi, Y. Khusanova et al., *The ALPINE-ALMA [CII] survey. Dust attenuation properties and obscured star formation at z ~ 4.4-5.8*, *Astronomy and Astrophysics* **643** (2020) A4 [2004.10760].

[34] Bogdanoska and Burgarella, *UV dust attenuation as a function of stellar mass and its evolution with redshift*, *Monthly Notices of the Royal Astronomical Society* **496** (2020) 5341.

[35] S. Schulz, G. Popping, A. Pillepich, D. Nelson, M. Vogelsberger, F. Marinacci et al., *A redshift-dependent IRX-β dust attenuation relation for TNG50 galaxies*, *Monthly Notices of the Royal Astronomical Society* **497** (2020) 4773.